Carbon nanotube film synthesized from ethanol and its oxidation behavior in air*

Ren Yan(任 彦)[a)b)], Ma Wen-Jun(马文君)[a)b)], Zeng Qing-Sheng(曾庆圣)[a)], Li Jin-Zhu(李金柱)[a)b)], Dong Hai-Bo(董海博)[a)b)], and Zhou Wei-Ya(周维亚)[a)†]

[a)] *Beijing National Laboratory of Condensed Matter Physics, Institute of Physics, Chinese Academy of Sciences, Beijing* 100190, *China*

[b)] *Graduate University of Chinese Academy of Sciences, Chinese Academy of Sciences, Beijing* 100039, *China*

(Received 6 May 2012)

In this paper, we propose an efficient way to synthesize carbon nanotube films using ferrocene and ethanol. The as-grown film is free-standing, semi-transparent, and of macro scale size. The tubes in the film are mostly single- or double-walled. The oxidation behavior of the film is studied via Raman spectroscopy, and the result indicates that the inner wall of the double-walled tube is effectively protected from oxidation by the outer wall.

Keywords: carbon nanotube, film, Raman spectroscopy, oxidation

PACS: 81.07.De, 81.15.Gh, 78.67.Ch, 61.48.De **DOI:** 10.1088/1674-1056/21/9/098103

1. Introduction

Since its discovery in 1991,[1] carbon nanotubes (CNTs) have been drawing the interest of scientists worldwide due to its unique physical properties and potential applications.[2] Carbon nanotube films, as a kind of macro structure of carbon nanotubes, are more convenient to handle with than the individual tubes or small bundles of tubes in nano-scale. The film structures of the tubes preserve some excellent properties of CNTs and have many potential applications.[3−11] Nowadays, the film can be obtained by filtration deposition of carbon nanotube solutions,[12] drawing vertically aligned CNT array,[13] or by chemical vapor deposition process.[14−16]

In this paper, we report a new method to synthesis macro scale films of CNTs based on the chemical vapor deposition (CVD) technique, in which ethanol is used as the carbon feeding source and ferrocene serves as the catalyst precursor. During the growth and deposit process, tubes would assemble into a film automatically. This is a more economic and more efficient way to obtain carbon nanotube films comparing with the other existing methods.[12−16] We analyze the influence of ethanol feeding rate on the final films and find that more carbon feeding would lead to more layers of tubes in the films. We also investigate the oxidation behavior of the as-grown film in the air by using the Raman spectroscopy, and the results indicate that the inner tubes of the coaxial tubes are protected by the outer ones during the oxidizing process.

2. Experiments

In our experiments, we use a home-made CVD equipment to synthesize the films. The basic setup of our CVD system is shown in Fig. 1. It mainly consists of a two-stage furnace and a control system of gas flow and temperature. Ethanol in a glass bottle is water-bathed, and the resulting vapor is carried into furnace A by Ar carrier gas (as indicated by the black arrows). The catalyst precursor (ferrocene) is placed in furnace A, where it is heated up and sublimated. The mixture of ethanol vapor and sublimated ferrocene is carried into furnace B by another argon flow with a larger flow rate. In furnace B, ethanol is subjected to pyrolysis at 1100 °C to grow carbon nanotubes. The temperature of water-bath is 30–50 °C. The temperature of furnace A is around 100 °C. The carrier gas flow rate for the ethanol vapor can be varied from 15 sccm to 150 sccm, and that for the mixture of ethanol vapor and sublimated ferrocene is ∼ 500 sccm.

*Project supported by the National Basic Research Program of China (Grant No. 2005CB623602) and the Key Item of Knowledge Innovation Project of Chinese Academy of Sciences (Grant No. KJCX2-YW-M01).

†Corresponding author. E-mail: wyzhou@aphy.iphy.ac.cn

© 2012 Chinese Physical Society and IOP Publishing Ltd

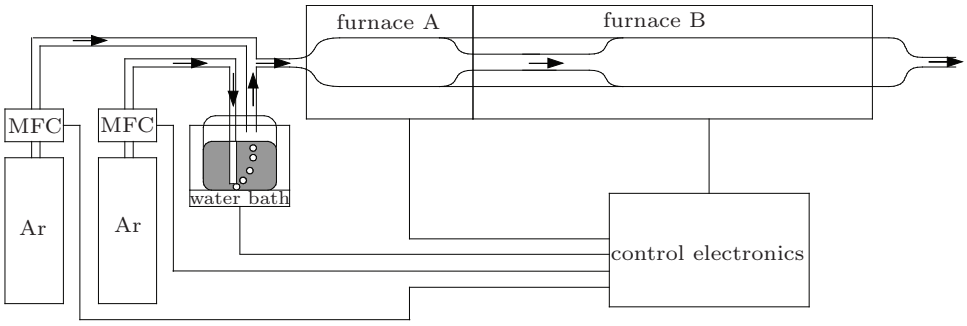


Fig. 1. Experimental setup for synthesis of the film. In furnace A, the catalyst is sublimated and then transported into furnace B carried by the mixture flow of argon and ethanol vapor.

The as-grown film adheres to the inner surface of the quartz tube and can be peeled off easily to obtain a free-standing film. We analyze the films by using scanning electron microscopy (SEM), transmission electron microscopy (TEM), and Raman microscopy. Figure 2(a) shows an optical image of the film, from which we can see that the film is semi-transparent and homogeneous over several square inches. The SEM image in Fig. 2(b) shows the structure of the film, which is constituted of highly entangled nanotube bundles. Figure 2(c) is a TEM image of the film. We can identify the diameters and the walls of the nanotubes in the film. A rough analysis from some TEM images shows that the tubes in the film are mainly single- or double-walled, and there also exist a very small amount of triple-walled tubes. The diameters of the tubes range from 0.9 nm to 2.5 nm. This result is in general agreement with the estimation from the Raman spectra.

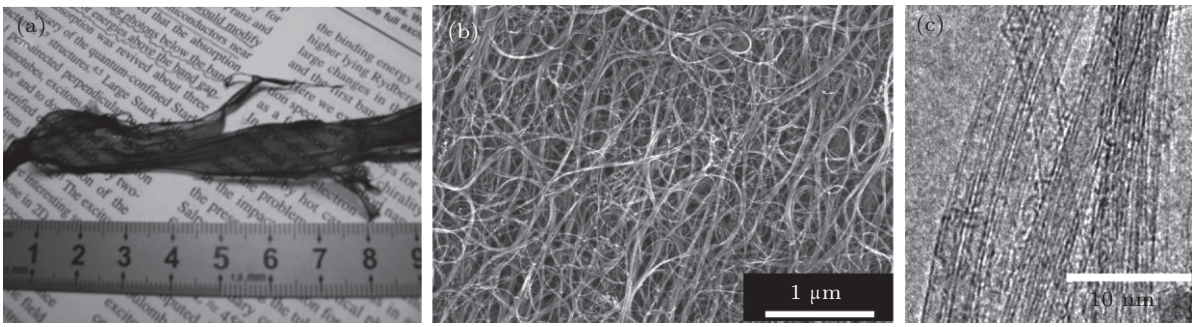


Fig. 2. The morphology of as-grown film. Panel (a) is an optical image, which shows that the film is semi-transparent; panel (b) is an SEM image of the film surface; and panel (c) is a TEM image showing the double-walled tubes in the bundles.

3. Results and discussion

We analyze the Raman spectra of the films grown under different ethanol feeding rates. The spectra are obtained with a Raman microscopy using 514 nm and 633 nm lasers. The results are shown in Fig. 3.

For all spectra shown in Fig. 3, the peaks around 180 cm^{-1} and 210 cm^{-1} are most intense, this can be attributed to the single-walled tubes with diameters around 1.3 nm and 1.1 nm. According to the Kataura plot (Fig. 4),[3,17] the energy gaps of nanotubes with these diameters (d_t) match with the photon energy of the incident laser (2.41 eV), and the intensity is enhanced by the resonance.

The difference between Figs. 3(a) and 3(b) is significant. The dominating peaks around 180 cm^{-1} in Fig. 3(a) decrease greatly when the carrier gas flow rate for ethanol is doubled from 50 sccm to 100 sccm, at the same time, the peaks around 210 cm^{-1} and 250 cm^{-1} arise. Figures 3(b) and 3(c) are very similar except that the peak around 160 cm^{-1} decreases. This indicates that the ratio of tubes around 1.5 nm decreases. Since the intensities for tubes with big diameters are usually very weak, this limits our observation to tubes with diameters smaller than 2 nm. From the analysis above, we can conclude that as the carbon

feed rate increases, the ratio of tubes around 1.3 nm decreases, and smaller tubes are enriched.

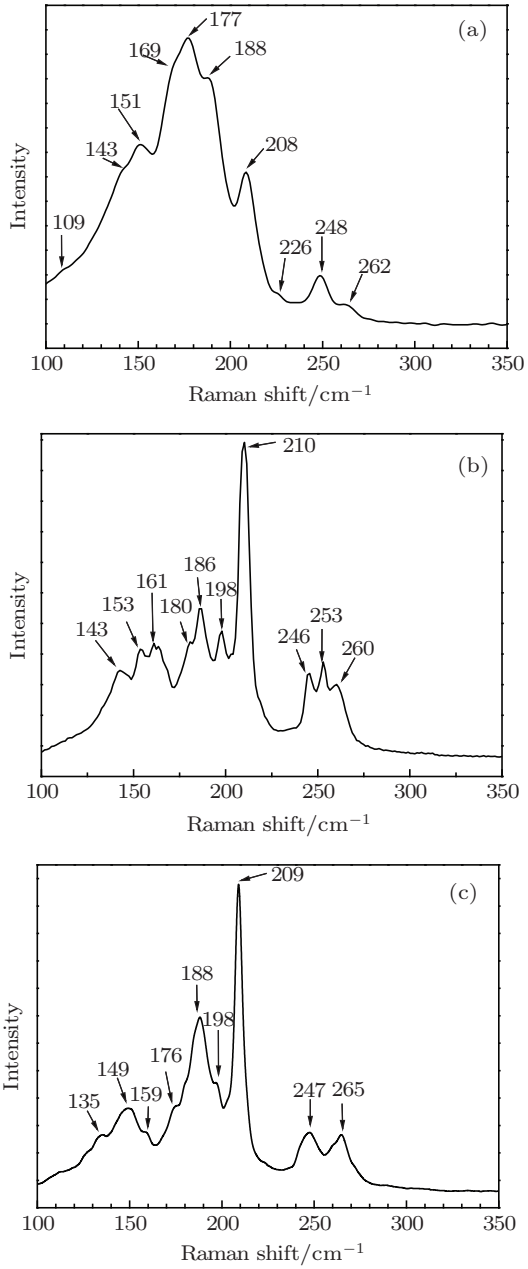


Fig. 3. Raman spectra of films grown under different ethanol feeding rates. The laser wavelength is 514 nm. For the spectra shown in panels (a), (b), and (c), the carrier gas flow rates for ethanol are 50 sccm, 100 sccm, and 150 sccm, respectively. The other growth parameters are all kept unchanged.

According to the TEM images, there are many double-walled tubes in our samples. We can assign the peaks above 200 cm^{-1} to the inner tubes, and the others to the outer tubes of the double-walled tubes and the single-walled tubes. Judging from the RBM frequencies, the diameters of the inner tubes are within 0.9–1.3 nm, while the outer tubes are above 1.7 nm in diameter, this result is in accord with our TEM results. Based on this assignment, we can further conclude that when we increase the carbon feed rate, the ratio of double-walled tubes in the as-grown film increases.

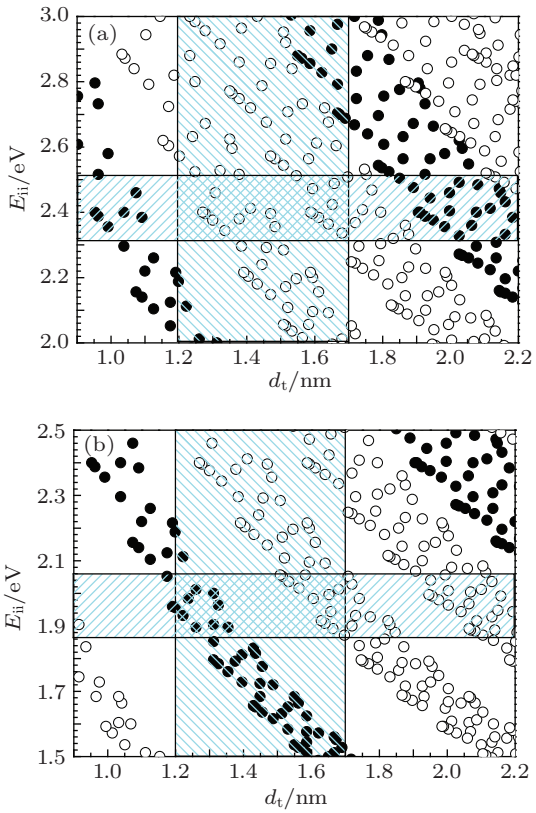


Fig. 4. (colour online) The Kataura plot for nanotubes. In this figure, open circles denote semiconductor tubes, and solid circles denote metallic tubes, the laser wavelengths are 514 nm (2.41 eV) in panel (a) and 633 nm (1.96 eV) in panel (b).

In order to investigate the oxidation behavior of such a film, we cut the film grown under 50 sccm ethanol feeding rate into many smaller pieces, and then expose the pieces in air at different temperatures for one hour. Finally, the Raman spectra of those pieces are collected and analyzed. During the whole signal collecting process, the configuration of the microscope is kept unchanged in order to compare the Raman spectra collected from different samples.

Figure 3(a) gives the original spectrum of the as-grown film under 514 nm laser, which is a very typical RBM profile. Figure 5(a) is the spectrum obtained after the 400 °C oxidization in air, which shows little variation except for the peak around 180 cm^{-1}. Figure 5(b) shows the spectrum obtained after the 520 °C oxidization in air, from which we can see that two holes appear in the profile. Figure 5(c) is the spectrum of the sample oxidized at 640 °C, which shows a further

hole-burning behavior.

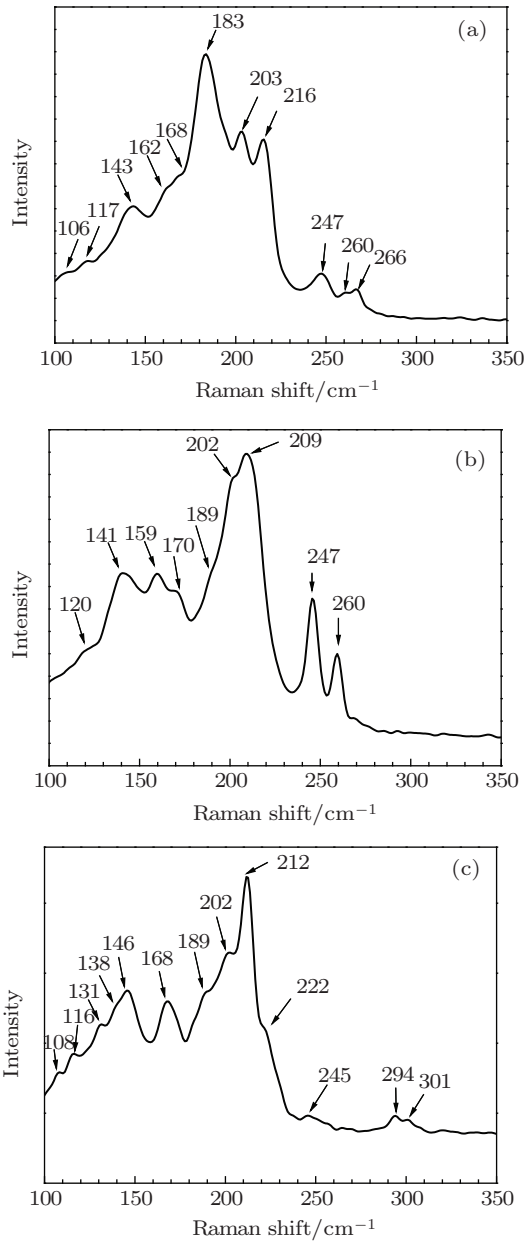


Fig. 5. Raman spectra of samples oxidized at (a) 400 °C, (b) 520 °C, and (c) 640 °C for one hour. The laser wavelength is 514 nm.

It is commonly accepted that smaller diameter tubes are more active and easier to be burned since the large curvature of the graphene layer.[18,19] But the above hole-burning behavior indicates that some bigger tubes are oxidized, while the smaller tubes survive. Since there are many double-walled tubes in our film, this phenomenon can be explained by the protection provided by the outer layers to the inner layers of the double-walled tubes.

Unlike the case of *in situ* oxidation,[20] our samples are exposed for oxidation for long enough time, thus if the outer layer of a double-walled tube has been corrupted, its inner layer should also have been oxidized. The tubes in the final samples are all in their original structures. From the estimation formula[21] $d = 248/\omega$, the peaks around 180 cm^{-1} are corresponding to the tubes with the diameter of about 1.3 nm. In Fig. 5(a), the peak weaken is caused by the oxidation of tubes with this diameter. When further oxidized, the tubes with larger diameters begin to be oxidized, the low frequency part of Fig. 5(b) shows this tendency. At the same time, the high frequency end raises, which indicates that the ratio of small diameter tubes raises.

Figure 6 gives the Raman spectra of the same samples obtained with the 633 nm laser. Figure 6(a) gives the spectrum of the original film, and figures 6(b), 6(c), and 6(d) give the spectra of samples after 400 °C, 520 °C, and 640 °C oxidation, respectively. The difference in the Raman profiles shown in Fig. 6 is not as significant as that in Fig. 5. The peaks around 140 cm^{-1} and 210 cm^{-1} are always the strongest during the oxidation processes. These two peaks are corresponding to the tubes with the diameters of 1.8 nm and 1.1 nm, respectively. They are kept uncorrupted during the oxidation.

The peaks around 180 cm^{-1} and 245 cm^{-1}, which appear under the 514 nm laser, are very weak here. They are corresponding to the tubes with the diameters of 1.3 nm and 1.0 nm, respectively. According to the Kataura plot, the tubes with diameter 1 nm will not resonate with the incident laser (1.96 eV) here, and the tubes with diameter 1.3 nm will resonate with the 633 nm laser if they are metallic (see Fig. 4(b)). Thus we may infer that the tubes with diameter around 1.3 nm in our samples are mainly semi-conductive.

In both Figs. 5 and 6, there exists such a tendency that the intensities of peaks around 165 cm^{-1} increase with the increase of the oxidation temperature, while the intensities of peaks around 155 cm^{-1} show a sign of decrease. This indicates that there are inner tubes around 1.4 nm and single walled tubes around 1.5 nm. As the temperature increases, the latter will be oxidized.

From the analysis above, we can draw a conclusion that the single-walled tubes are oxidized gradually and the remaining small diameter tubes are the inner tubes of the double-walled tubes. They are protected from oxidation by their outer layers.

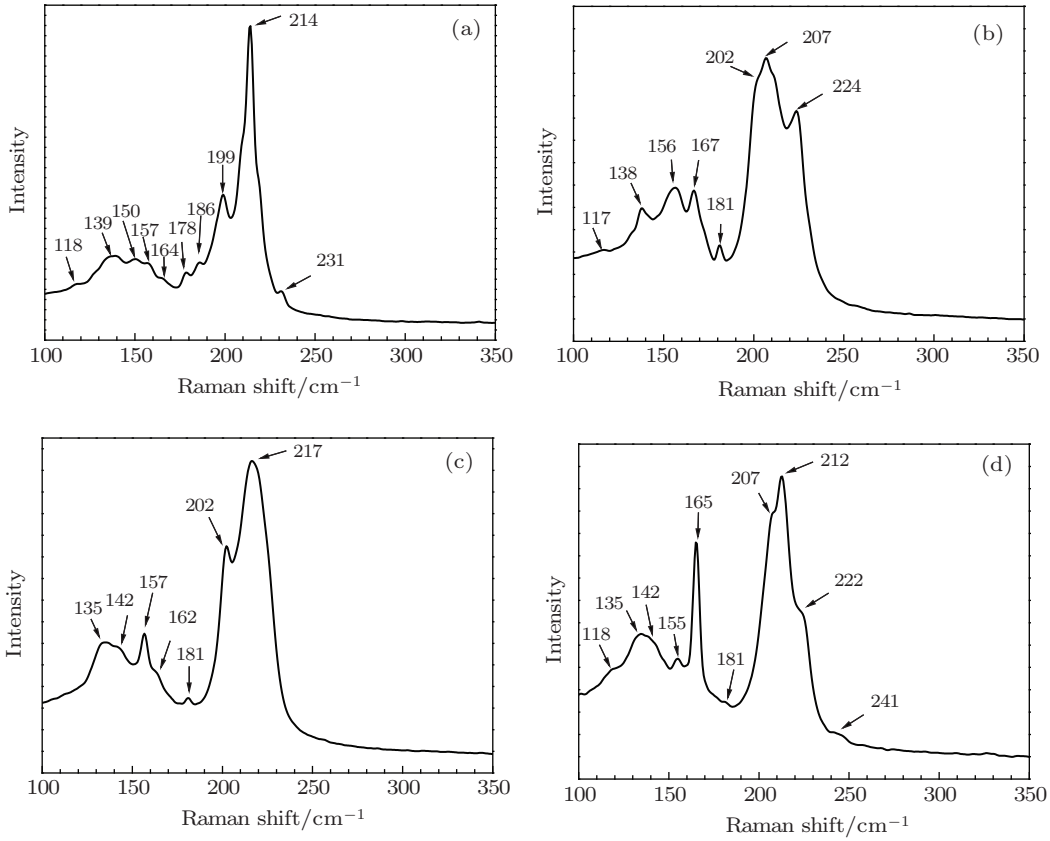


Fig. 6. Raman spectra of sample oxidized under different temperatures ((a) original, (b) 400 °C, (c) 520 °C, (d) 640 °C) for an hour. The laser wavelength is 633 nm.

4. Conclusion

In summary, we synthesized a macro scale carbon nanotube film directly from ethanol and characterized the as-grown film in many measures. We found that the carbon feeding rate would alter the diameters of the nanotubes and the ratios of single- and double-walled tubes in the film. The oxidation behavior in air of the film was also investigated by using the Raman spectroscopy, and the results indicated that the inner tubes were effectively screened from oxidation by the outer tubes.

Acknowledgments

The authors would like to thank Professor Tan P H, Professor Guo Y J, and Ms. Zhu K for Raman measurements, Ms. Wang C Y for SEM characterization, Mr. Yang X A for TEM characterization.

References

[1] Iijima S 1991 *Nature* **354** 56

[2] Saito R, Dresselhaus G and Dresselhaus M 1998 *Physical Properties of Carbon Nanotubes* (London: Imperial College Press) p. 5

[3] Tatsuura S 2003 *Adv. Mater.* **15** 534

[4] Dharap P, Li Z, Nagarajaiah S and Barrera E V 2004 *Sensor Review* **24** 271

[5] Itkis M E, Borondics F, Yu A P and Haddon R C 2006 *Science* **312** 413

[6] Lee K 2004 *Nano Lett.* **4** 911

[7] Snow E S, Perkins F K, Houser E J, Badescu S C and Reinecke T L 2005 *Science* **307** 1942

[8] Zhang D, Ryu K, Liu X, Polikarpov E, Ly J, Tompson M and Zhou C 2006 *Nano Lett.* **6** 1880

[9] Liu L Q, Ma W J and Zhang Z 2011 *Small* **7** 1504

[10] Song L, Liu S, Zhang G M, Liu L F, Ma W J, Liu D F, Zhao X W, Luo S D, Zhang Z X, Xiang Y J, Shen J, Zhou J J, Wang G and Zhou W Y 2006 *Chin. Phys.* **15** 422

[11] Niu Z Q, Ma W J, Dong H B, Li J Z and Zhou W Y 2011 *Chin. Phys.* B **20** 028101

[12] Wu Z, Chen Z, Du X, Logan J M, Sippel J, Nikolou M, Kamaras K, Reynolds J R, Tanner D B, Hebard A F and Rinzler A G 2004 *Science* **305** 1273

[13] Jiang K L, Wang J P, Li Q Q, Liu L, Li C H and Fan S S 2011 *Adv. Mater.* **23** 1154

[14] Ma W J, Song L, Yang R, Zhang T H, Zhao Y C, Sun L F, Ren Y, Liu D F, Liu L F, Shen J, Zhang Z X, Xiang Y J, Zhou W Y and Xie S S 2007 *Nano Lett.* **7** 2307

[15] Zhou W Y, Ma W J, Niu Z Q, Song L and Xie S S 2011 *Chinese Science Bulletin* **57** 205

[16] Liu Q, Ren W, Wang D W, Chen Z G, Pei S, Liu B, Li F, Cong H, Liu C and Cheng H M 2009 *ACS Nano* **3** 707

[17] Kataura H, Kumazawa Y, Maniwa Y, Umezu I, Suzuki S, Ohtsuka Y and Achiba Y 1999 *Synthetic Metals* **103** 2555

[18] Niyogi S, Hamon M A, Hu H, Zhao B, Bhowmik P, Sen R, Itkis M E and Haddon R C 2002 *Acc. Chem. Res.* **35** 1105

[19] Xu X and Kang H 2007 *Chem. Mater.* **19** 3767

[20] Osswald S, Flahaut E and Gogotsi Y 2006 *Chem. Mater.* **18** 1525

[21] Kurti J, Kresse G and Kuzmany H 1998 *Phys. Rev.* B **58** 8869